Research Square

Preprints are preliminary reports that have not undergone peer review.
They should not be considered conclusive, used to inform clinical practice,
or referenced by the media as validated information.

White-Light Spectral Interferometry for Thin-Film Thickness and Group-Index Dispersion Metrology

Shouvik Sadhukhan

shouvikphysics1996@gmail.com

Indian Institute of Space Science and Technology https://orcid.org/0000-0002-0332-0371

Shirsendu Sarkar

West Bengal State University

Debabrata Bhadra

West Bengal State University

Research Article

Keywords: White-light interferometry, spectral interferometry, thin-film thickness, group refractive index, equalization wavelength, channeled spectrum, BK7, SiO2/Si, Levenberg--Marquardt fitting

Posted Date: October 5th, 2026

DOI: https://doi.org/10.21203/rs.3.rs-11242029/v1

License: This work is licensed under a Creative Commons Attribution 4.0 International License.
Read Full License

Additional Declarations: The authors declare no competing interests.

White-Light Spectral Interferometry for Thin-Film Thickness and Group-Index Dispersion Metrology

Shirsendu Sarkar[1], Shouvik Sadhukhan[2], Debabrata Bhadra[3]

[1]Dept. of Physics, West Bengal State University, Barasat, India
[2]Applied and Adaptive Optics Laboratory, Dept. of Physics, IIST, Trivandrum, India
[3]Dept. of Physics, Bhairab Ganguly College, Kolkata, India

October 1, 2026

Abstract

Unified study of two complementary metrology tasks

Thickness of a thin film on a substrate, and group-refractive-index dispersion of an optical element, both from the **channeled spectrum** of a slightly dispersive Michelson interferometer recorded by a fiber-optic spectrometer (framework of Hlubina and co-workers).

Thin film: SiO_2/Si, 100–450 nm

- Model R, V, δ_r, ϕ_{nl}
- Levenberg–Marquardt (LM) fit of noisy spectra
- Errors within ± 0.2 nm; $R > 0.998$
- χ^2 scan: single sharp minimum at true d

Dispersion: uncompensated BK7 beam splitter

- Equalization condition $N_g(\lambda_{\mathrm{eq}}) = \Delta L/t + 1$
- 35 interferograms, $\Delta L = 10.990$–11.709 mm
- $\lambda_{\mathrm{eq}} = 480$–$860$ nm; $N_g = 1.558 \rightarrow 1.525$ (Sellmeier-consistent)
- $\Delta L = 11.30$ mm: $\lambda_{\mathrm{eq}} = 598.5$ nm, $N_g = 1.5401$
- $n(\lambda)$ recovered from N_g to 7×10^{-9} (noiseless)

Scan-free, single-instrument approach to thin-film and dispersion metrology.

Outline

1. Motivation and background
2. Theory
   - Channeled spectrum, visibility, OPD
   - Sellmeier model of BK7
   - Thin-film reflection and phase
   - Equalization wavelength
   - Phase-index reconstruction
   - LM fitting and χ^2
3. Experiments and simulation methodology
4. Results
   - SiO_2/Si thickness retrieval
   - BK7 group-index dispersion
   - Phase-index reconstruction
5. Precision and systematic effects
6. Conclusions
7. References

Motivation and Background

- The channeled spectrum at the output of a two-beam interferometer carries the full phase information of the interfering waves; linked to coherence-induced spectral changes and spectral shifts/switches near phase singularities [Wolf86, JW91, Pu04, Brun07, Gbur01, Foley02].
- Studied in dispersive two-beam interferometers [Hlu97, Kov99, Hlu00a, Hlu00b, Hlu01a], optical fibres [Tat81, Did96, Lee06]; relevant to displacement sensing and fiber-optic gyroscopes [Tap01, Khi18].
- Phase extraction: Fourier-transform, wavelet, least-squares [Dor00, Reo06, Deng09].

Two key applications sharing one instrument and one expression

1. **Thin film:** one arm ends at a film structure; reflectance and nonlinear phase modulate fringe visibility and phase, so d follows from a single spectrum, no scanning [Hlu01FS, Hlu04, Hlu07].
2. **Uncompensated Michelson:** beam splitter imbalance $\propto N_g$; the envelope peak λ_{eq} shifts with mirror displacement and yields $N_g(\lambda)$ [Hlu00b, Hlu01FS].

This work: common notation and model; LM thickness retrieval (100–450 nm); equalization condition, 35 interferograms, $n(\lambda)$ reconstruction; precision discussion.

Theory I: Channeled Spectrum of a Dispersive Michelson Interferometer

Spatially coherent white light; glass beam splitter of thickness t, indices $n(\lambda)$, $N_g(\lambda)$; spectrometer with Gaussian response width $\Delta\lambda_R$ [Hlu07, Hlu04]:

$$I(\lambda) = I^{(0)}(\lambda)\left\{1 + V(\lambda)\exp\left[-\frac{\pi^2}{2}\left(\frac{\Delta^g(\lambda)\Delta\lambda_R}{\lambda^2}\right)^2\right]\cos\left[\frac{2\pi}{\lambda}\Delta(\lambda)\right]\right\} \tag{1}$$

- $I^{(0)}$: reference spectrum (source $\times$ broadband reflectance, fringes unresolved)
- $V(\lambda)$: visibility; $\Delta(\lambda)$: phase OPD; $\Delta^g(\lambda)$: group OPD
- Exponential: contrast loss from finite resolution; $\to 1$ for $\Delta\lambda_R \to 0$

Visibility (arm ends at reflectance R):

$$V(\lambda) = V_I\,\frac{2\sqrt{R(\lambda)}}{1 + R(\lambda)} \tag{2}$$

$V_I \leq 1$: polarization mismatch, coherence, alignment.
Two ideal mirrors: $V = V_I = 1$.

Phase OPD:

$$\Delta(\lambda) = 2L + 2n(\lambda)t - \frac{\lambda\,\delta_r(\lambda)}{2\pi} \tag{3}$$

$2L$: air path difference (air dispersion neglected); δ_r: phase change on reflection (=const for a metallic mirror).

Theory II: Group OPD, Group Index and Sellmeier Model

Group OPD (stationary phase, $\Phi = 2\pi\Delta/\lambda$, $\mathrm{d}\Phi/\mathrm{d}(1/\lambda)$; group delay on reflection neglected):

$$\Delta^g(\lambda) \approx 2L + 2N_g(\lambda)\, t \tag{4}$$

Group index:

$$N_g(\lambda) = n - \lambda\frac{\mathrm{d}n}{\mathrm{d}\lambda}, \qquad N_g(\omega) = n + \omega\frac{\mathrm{d}n}{\mathrm{d}\omega} \tag{5}$$

It contains both the phase index and its dispersion slope.

Differentiating:

$$\frac{\mathrm{d}n}{\mathrm{d}\lambda} = -\frac{\lambda}{n}\sum_{i=1}^{3}\frac{B_i C_i}{(\lambda^2 - C_i)^2}, \qquad N_g(\lambda) = n + \frac{\lambda^2}{n}\sum_{i=1}^{3}\frac{B_i C_i}{(\lambda^2 - C_i)^2} \tag{7}$$

Evaluated numerically at any visible/NIR wavelength.

BK7 three-term Sellmeier (λ in μm, 20 °C):

$$n^2(\lambda) = 1 + \sum_{i=1}^{3}\frac{B_i\lambda^2}{\lambda^2 - C_i} \tag{6}$$

$B_1 = 1.03961212$, $B_2 = 0.231792344$, $B_3 = 1.01046945$
$C_1 = 6.00069867 \times 10^{-3}$, $C_2 = 2.00179144 \times 10^{-2}$,
$C_3 = 1.03560653 \times 10^{2}\ \mu\mathrm{m}^2$

Theory III: Reflection from a Thin-Film Structure

Normal incidence; film (medium 1, $\tilde{n}_1 = n_1 - i\kappa_1$, thickness d) on substrate (medium 2, $\tilde{n}_2 = n_2 - i\kappa_2$) in air. Fabry–Perot summation [Hlu07]:

$$r(\lambda) = \frac{r_{01} + r_{12}\, e^{i2\beta}}{1 + r_{01} r_{12}\, e^{i2\beta}}, \qquad r_{01} = \frac{1 - \tilde{n}_1}{1 + \tilde{n}_1}, \quad r_{12} = \frac{\tilde{n}_1 - \tilde{n}_2}{\tilde{n}_1 + \tilde{n}_2}, \quad \beta = \frac{2\pi}{\lambda}\tilde{n}_1 d \tag{8}$$

Writing $r = \sqrt{R}\, e^{i\delta_r}$: power reflectance $R = |r|^2$ and phase change on reflection

$$\delta_r(\lambda) = \frac{2\pi}{\lambda}\, 2n_1(\lambda)\, d + \phi_{\mathrm{nl}}(\lambda) \tag{9}$$

linear (geometrical) term + nonlinear phase ϕ_{nl} from multiple internal reflections $\Rightarrow$ spectral anomalies beyond a simple mirror.

Optical constants of SiO_2/Si

$$n_1^2(\lambda) = 1 + \frac{A\lambda^2}{\lambda^2 - \lambda_s^2}, \qquad A = 1.1336, \quad \lambda_s = 9.261 \times 10^{-2}\,\mu\mathrm{m} \tag{10}$$

SiO_2: negligible extinction in the visible. Si (absorbing): complex index from Palik tables [Palik95].

Theory IV: Equalization Wavelength and Group-Index Extraction

Uncompensated arm longer by $(N_g - 1)t$ in group path; ΔL: extra air path (mirror displacement). With $L = -(\Delta L + t)$ and constant δ_r:

$$\mathrm{OPD}(\lambda) = -2\Delta L + 2[n(\lambda) - 1]t, \qquad \mathrm{OPD}_g(\lambda) = -2\Delta L + 2[N_g(\lambda) - 1]t \tag{11}$$

Envelope maximal at λ_{eq} where $\mathrm{OPD}_g(\lambda_{\mathrm{eq}}) = 0$:

$$\boxed{N_g(\lambda_{\mathrm{eq}}) = \frac{\Delta L}{t} + 1} \tag{12}$$

- Measure λ_{eq} for known ΔL, $t \Rightarrow N_g(\lambda_{\mathrm{eq}})$ directly; varying ΔL traces $N_g(\lambda)$.
- With Sellmeier, solve numerically for $\lambda_{\mathrm{eq}}(\Delta L)$; N_g decreases monotonically in the visible $\Rightarrow$ unique solution.
- Larger $\Delta L \Rightarrow$ larger $N_g \Rightarrow$ shorter λ_{eq} (blue shift).

Effective beam-splitter thickness (if t unknown)

$$\frac{\mathrm{d}N_g}{\mathrm{d}(\Delta L)} = \frac{1}{t}, \qquad N_g^{\mathrm{meas}}(\lambda_{\mathrm{eq}}^{(j)}) = N_g^{\mathrm{Sell}}(\lambda_{\mathrm{eq}}^{(j)}) + \epsilon_j, \quad \min \sum_{j=1}^{M} \epsilon_j^2 \tag{13}$$

Slope of N_g vs. ΔL, or least-squares fit to Sellmeier (optionally with zero offset ΔL_0).

Theory V: Phase-Index Reconstruction from Group-Index Data

$N_g = n - \lambda\, \mathrm{d}n/\mathrm{d}\lambda$ is a first-order linear ODE:

$$\frac{\mathrm{d}n}{\mathrm{d}\lambda} - \frac{n}{\lambda} = -\frac{N_g(\lambda)}{\lambda} \tag{14}$$

Integrating factor $\mu = 1/\lambda$ gives $\mathrm{d}(n/\lambda)/\mathrm{d}\lambda = -N_g/\lambda^2$, hence

$$\boxed{n(\lambda) = -\lambda \int \frac{N_g(\lambda)}{\lambda^2}\, \mathrm{d}\lambda + C\lambda} \tag{15}$$

Discrete data $\{\lambda_i, N_g(\lambda_i)\}$:

$$n(\lambda_i) = \lambda_i \left[C - \sum_{j=1}^{i} \frac{N_g(\lambda_j)}{\lambda_j^2}\, \Delta\lambda \right] \tag{16}$$

- C must be fixed by a boundary condition: known $n(\lambda_0)$, independent ellipsometry, or a dispersion model; otherwise infinitely many solutions.
- Useful when only group-delay measurements are available.

Theory VI: Figure of Merit and Levenberg–Marquardt Fitting

Thickness d, instrumental visibility V_I and air path difference L are recovered by minimizing

$$\chi^2(V_I, L, d) = \sum_{i=1}^{N} \left[I^e(\lambda_i) - I(\lambda_i; V_I, L, d) \right]^2 \tag{17}$$

- $I^e(\lambda_i)$: recorded (or simulated) spectrum; $I(\lambda_i; V_I, L, d)$: model of Eq. (1) at N points over 450–900 nm.
- **Levenberg–Marquardt** [Hlu07, Press07]: blends gradient descent and Gauss–Newton steps; converges reliably from physically reasonable initial guesses.
- Fit quality: Pearson correlation coefficient R between measured and fitted spectra.

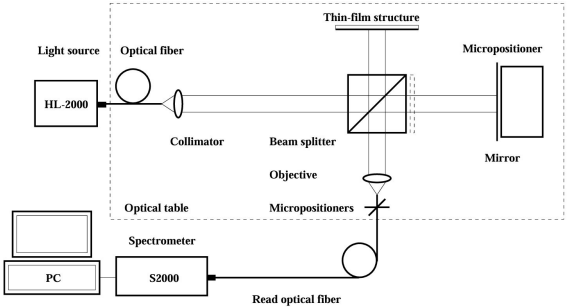
Workflow

Synthetic spectrum (known d, V_I, L) $\rightarrow$ add 1% Gaussian noise $\rightarrow$ LM fit $\rightarrow$ compare d_{fit} with d_{true} $\rightarrow$ scan $\chi^2(d)$ for uniqueness of the minimum.

Experiment I: Thin-Film Configuration

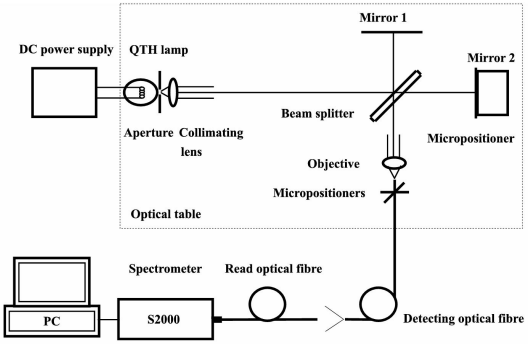
- Bulk-optic Michelson; halogen HL-2000 source (Ocean Optics) $\rightarrow$ multimode fiber $\rightarrow$ collimator
- BK7 cube beam splitter, $t_{\text{eff}} = -10.10\,\mu$m (found independently by spectral interferometry [Hlu07])
- One arm: metallic mirror on micropositioner; other arm: SiO_2/Si sample on micropositioner
- Microscope objective + micropositioners $\rightarrow$ read fiber $\rightarrow$ S2000 spectrometer, Gaussian response $\Delta\lambda_R = 3\,$nm $\rightarrow$ PC

Simulation: synthetic spectra from Eq. (1), known d, V_I, L; Gaussian noise, $\sigma = 1\%$ of peak; LM retrieval as for real data; 8 samples, $d = 100$–$450\,$nm, $50\,$nm steps.



Experiment II: Uncompensated Michelson for Group-Index Dispersion

- **Illumination:** QTH lamp, stabilized DC supply; adjustable aperture (spatial filtering, higher coherence); collimating lens.
- **Interferometer:** non-polarizing beam splitter at 45°; Mirror 1 on precision translation stage sets ΔL; Mirror 2 on high-resolution micropositioner for fine alignment.
- **Detection:** objective → detecting fiber → S2000 (or equivalent) → readout fiber → PC; micropositioners optimize fringe visibility; vibration-isolated table.
- **Procedure:** translate mirror in steps; record interferogram; read λ_{eq} from the envelope peak; obtain N_g from $N_g = \Delta L/t + 1$.



Simulation Methodology and Parameters

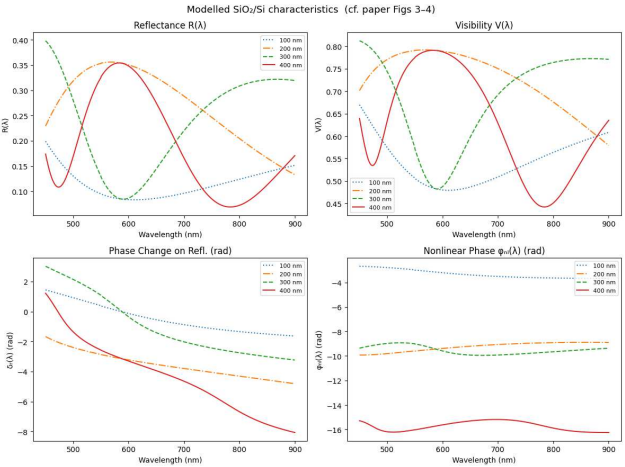
BK7 dispersion simulation

- $\Delta L \in [10.990, 11.709]$ mm, step ≈ 0.021 mm (35 values), $\lambda_{\mathrm{eq}} \approx 480$–$860$ nm
- Source spectrally flat, 500–860 nm; ideal spectrometer ($V = 1$, no resolution factor)
- Interferogram from Sellmeier n and $\mathrm{d}n/\mathrm{d}\lambda$
- Envelope = magnitude of analytic signal (Hilbert transform along λ); $\lambda_{\mathrm{eq}}^{(j)}$ = envelope-peak wavelength
- Operating point $\Delta L_0 = 11.30$ mm: $\lambda_{\mathrm{eq}} = 598.5$ nm, $N_g = 1.5401$; $t = \Delta L_0/(N_g - 1)$ at this point

Parameter	Thin film	BK7
Sample	SiO_2/Si, 100–450 nm	BK7 splitter
t	$t_{\mathrm{eff}} = -10.10\,\mu$m	see text
Window	450–900 nm	480–860 nm
Spectrometer	Gauss, $\Delta\lambda_R = 3$ nm	ideal
Noise	Gauss, 1% peak	none
Cases	8 thicknesses	35 displacements
Analysis	LM fit of χ^2	envelope peak

Principal simulation parameters of the two studies.

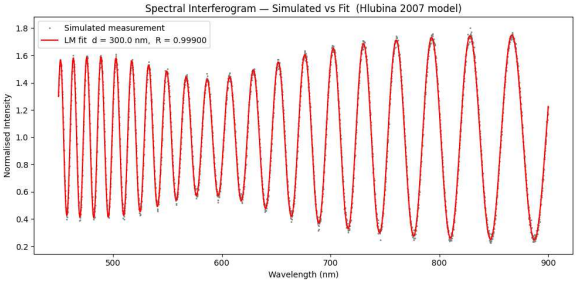
Results I: Optical Characteristics of SiO_2/Si

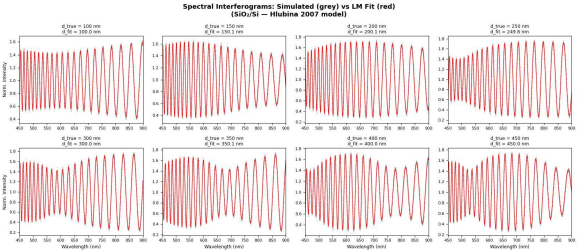


$d = 100$ (dotted), 200 (dash-dot), 300 (dashed), 400 nm (solid)

- $R(\lambda)$ oscillates; oscillation faster for thicker films (more phase β per unit λ).
- $V = V_I\, 2\sqrt{R}/(1+R)$ inherits the modulation: ≈ 0.45–0.80 across the visible.
- $\delta_r(\lambda)$ decreases monotonically; curvature grows with d.
- ϕ_{nl}: thickness-dependent offset (≈ -3 rad at 100 nm to ≈ -16 rad at 400 nm); flat for thin films, more structure as d grows.
- These distort the fringe envelope asymmetrically and encode d beyond the fringe period.

Results II: Simulated Interferograms and LM Fits



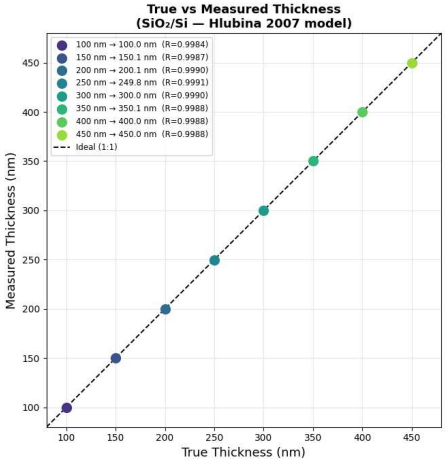


All eight samples, 450–900 nm

$d = 300\,\text{nm}$: $d_{\text{fit}} = 300.0\,\text{nm}$, $R = 0.99900$

- Fringes span 450–900 nm; visibility is wavelength dependent and increases toward the red, consistent with $R(\lambda)$.
- Fits uniformly excellent, $R > 0.998$. Fringe period is set mainly by the gross group OPD, so fringe count is similar in all panels; d appears as modulation of visibility and local phase, which the fit exploits.

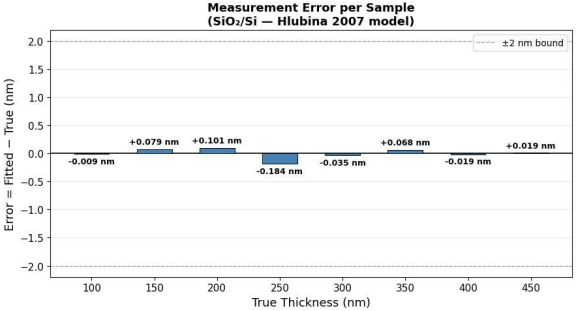
Results III: True vs. Retrieved Thickness



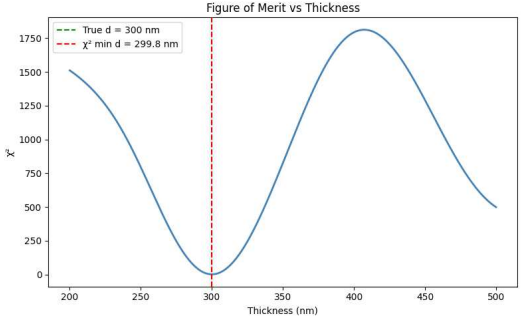
d_{true} (nm)	d_{fit} (nm)	Error (nm)	R
100	100.0	-0.009	0.9984
150	150.1	$+0.079$	0.9987
200	200.1	$+0.101$	0.9990
250	249.8	-0.184	0.9991
300	300.0	-0.035	0.9990
350	350.1	$+0.068$	0.9988
400	400.0	-0.019	0.9988
450	450.0	$+0.019$	0.9988

- Points lie on the ideal 1:1 line: linear and accurate.
- R from 0.9984 ($d = 100\,\mathrm{nm}$) to 0.9991 (250 nm).

Results IV: Error Analysis and χ^2 Landscape

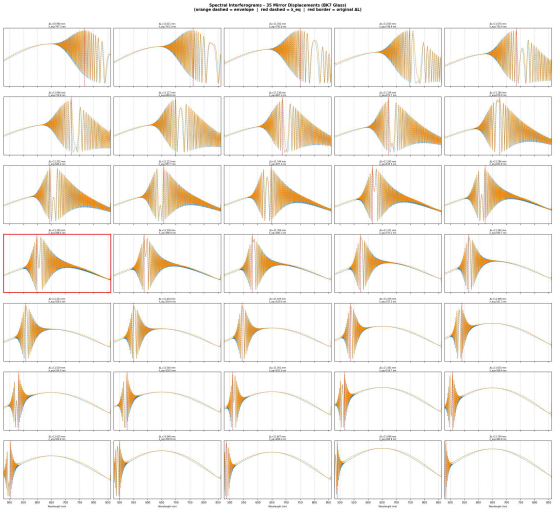


- All errors within ± 0.2 nm, over an order of magnitude below the ± 2 nm bound.
- Largest: -0.184 nm (250 nm); smallest: -0.009 nm (100 nm).
- No systematic trend $\Rightarrow$ noise-dominated, not model-limited.



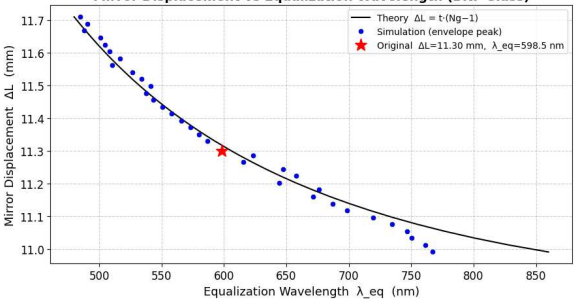
- $d_{\mathrm{true}} = 300$ nm, scan 190–500 nm, V_l, L at optimum.
- Single deep minimum at $d = 299.8$ nm; maximum near 410 nm; no competing minimum.
- Many fringes over 450–900 nm $\Rightarrow$ wrong phase/envelope gives large residuals; broader bandwidth $\Rightarrow$ narrower valley, higher precision [Hlu07].

Results V: BK7 Interferograms at 35 Mirror Displacements



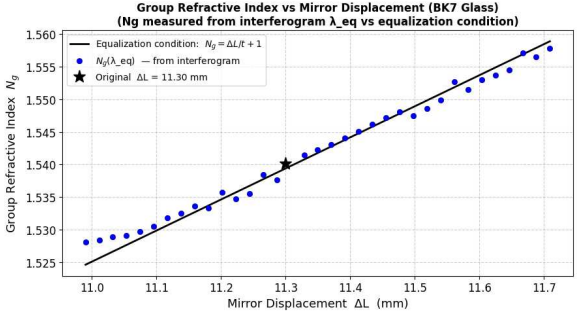
- $\Delta L = 10.990\,\text{mm}$ (upper left): $\lambda_{\text{eq}} = 787.3\,\text{nm}$
  $\Delta L = 11.709\,\text{mm}$ (lower right): $\lambda_{\text{eq}} = 484.8\,\text{nm}$
- Blue: interferogram; orange dashed: envelope; red dashed line: λ_{eq}.
  Red-bordered panel: $\Delta L = 11.30\,\text{mm}$, $\lambda_{\text{eq}} = 598.5\,\text{nm}$.
- Envelope peak migrates from NIR to shorter wavelengths as ΔL increases.
- $\Delta L > 11.5\,\text{mm}$: λ_{eq} in blue-green; red-side fringes tightly packed (stronger BK7 dispersion at short λ).
- $\Delta L < 11.1\,\text{mm}$: peak in NIR, broad slowly varying fringes on the blue side.

Results VI: ΔL and N_g vs. Equalization Condition



ΔL **vs.** λ_{eq}**:** theory $\Delta L = t[N_g(\lambda_{\mathrm{eq}}) - 1]$ (line), simulated envelope peaks (dots), operating point (star).

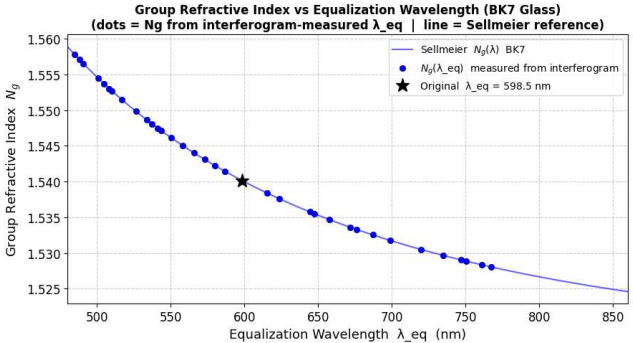
- Points follow the curve; largest scatter at long wavelengths.
- Monotonic decrease: longer $\lambda_{\mathrm{eq}} \leftrightarrow$ smaller ΔL.



N_g **vs.** ΔL**:** line of slope $1/t$; star: $\Delta L = 11.30\,\mathrm{mm}$, $N_g = 1.5401$.

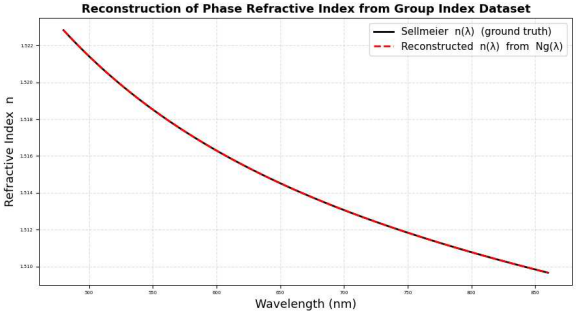
- Points follow the linear locus; deviations of a few 10^{-3} at the ends, notably $\Delta L < 11.1\,\mathrm{mm}$ (broad, hard-to-locate peak).
- Slope of a linear fit gives $1/t$, hence the effective t.

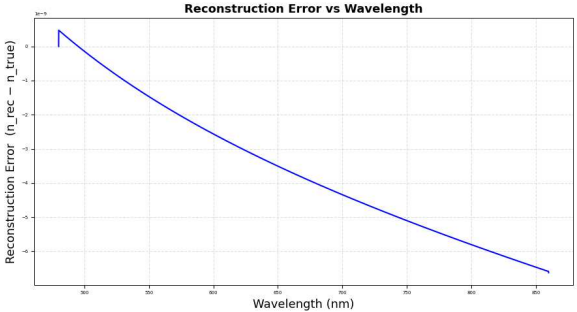
Results VII: Group Index vs. Equalization Wavelength



- Line: Sellmeier $N_g(\lambda)$; dots: N_g at interferogram-measured λ_{eq}; star: $\lambda_{\mathrm{eq}} = 598.5\,\mathrm{nm}$, $N_g = 1.5401$.
- $N_g \approx 1.558$ at $480\,\mathrm{nm} \rightarrow N_g \approx 1.525$ at $860\,\mathrm{nm}$: normal dispersion of BK7.
- Points sample the curvature of the Sellmeier curve over 480–860 nm: sensitive to dispersion beyond the linear slope.
- The three representations $\Delta L(\lambda_{\mathrm{eq}})$, $N_g(\Delta L)$, $N_g(\lambda_{\mathrm{eq}})$ are mutually consistent, supporting the equalization-wavelength framework.

Results VIII: Phase-Index Reconstruction





Reconstructed $n(\lambda)$ (red dashed) vs. Sellmeier (black)

$\Delta n = n_{\mathrm{rec}} - n_{\mathrm{Sellmeier}}$

- Numerical integration of the N_g data (Eqs. for $n(\lambda)$ and $n(\lambda_i)$): curves indistinguishable over 480–860 nm.
- $|\Delta n| \lesssim 7 \times 10^{-9}$; smooth and monotonic $\Rightarrow$ integration discretization, not model mismatch. Well conditioned for smooth dispersion such as BK7.
- Caveat: noiseless data with the boundary value taken from the model; shows mathematical consistency, not noise performance (real N_g precision $\sim 10^{-4}$).

Precision and Systematic Effects

Thin-film study

Precision limited by spectrum SNR, spectrometer resolution ($\Delta\lambda_R = 3\,\text{nm}$) and accuracy of assumed optical constants; in practice also micropositioner drift and vibration. Sub-nanometer accuracy is achievable in principle for SiO_2 films down to 100 nm if optical constants are well characterized.

Equalization-wavelength measurement (real experiment):

- **Spectrometer resolution:** finite $\delta\lambda$ broadens the envelope and shifts apparent λ_{eq} by $\sim (\delta\lambda)^2/\Lambda$ (Λ: local fringe period). For $\delta\lambda \approx 0.5\,\text{nm}$, $\Lambda \approx 5\,\text{nm}$: shift $< 0.05\,\text{nm}$.
- **Source spectrum:** non-flat spectrum modulates the envelope amplitude but does not shift λ_{eq} if the spectrometer is intensity-calibrated.
- **Beam-splitter inhomogeneity:** aperture-averaged $\bar{t}$; negligible for flats better than $\lambda/10$.
- **Mirror tilt/alignment:** wavelength-dependent phase gradient but no envelope-peak shift for small detector solid angle.

Precision in N_g of order 10^{-4} is attainable, consistent with fused silica [Hlu01FS]; both applications share the same error sources, so one instrument serves both.

Conclusions

Thin-film thickness (SiO_2/Si)

- Common channeled-spectrum model; R, V, δ_r, ϕ_{nl} modeled.
- LM fits of noisy spectra, 8 thicknesses (100–450 nm): errors within ± 0.2 nm, $R > 0.998$.
- χ^2 scan: single sharp minimum at true d.

Group-index dispersion (BK7)

- $N_g(\lambda_{\mathrm{eq}}) = \Delta L/t + 1$; 35 interferograms, $\Delta L = 10.990$–11.709 mm.
- $\lambda_{\mathrm{eq}} = 480$–$860$ nm; $N_g = 1.558 \rightarrow 1.525$, following Sellmeier.
- $\Delta L = 11.30$ mm: $\lambda_{\mathrm{eq}} = 598.5$ nm, $N_g = 1.5401$.
- $n(\lambda)$ recovered to 7×10^{-9} (noiseless).

Both need only a broadband source, a Michelson interferometer and a fiber-optic spectrometer: simple and suited to laboratory and industrial use.

Future work: multilayer structures, angle-resolved configurations, multilayer beam splitters, absorbing and birefringent materials, noisy experimental data; link to the spectral-anomaly framework relevant to gyroscopic and phase-singularity applications.

Funding: **DST/SERB, India (CRG/2020/003338)**.

References I

[Wolf86] E. Wolf, "Non-cosmological redshifts of spectral lines," *Nature* 326, 363–365 (1986).

[JW91] D.F.V. James and E. Wolf, "Some new aspects of Young's interference experiment," *Phys. Lett. A* 157, 6–10 (1991).

[Pu04] J. Pu, C. Cai, and S. Nemoto, "Spectral anomalies in Young's double-slit interference experiment," *Opt. Express* 12, 5131 (2004).

[Brun07] M.M. Brundavanam, N.K. Viswanathan and N.R. Desai, "Spectral anomalies due to temporal correlation in a white-light interferometer," *Opt. Lett.* 32, 2279–2281 (2007).

[Brun08] M.M. Brundavanam, N.K. Viswanathan and D.N. Rao, "Nanodisplacement measurement using spectral shifts in a white-light interferometer," *Appl. Opt.* 47, 6334–6339 (2008).

[Brun09] M.M. Brundavanam, N.K. Viswanathan and D.N. Rao, "Effect of input spectrum on the spectral switch characteristics in a white-light Michelson interferometer," *J. Opt. Soc. Am. A* 26, 2592–2599 (2009).

[Pu99] J. Pu, H. Zhang and S. Nemoto, "Spectral shifts and spectral switches of partially coherent light passing through an aperture," *Opt. Commun.* 162, 57–63 (1999).

[Gbur01] G. Gbur, T.D. Visser and E. Wolf, "Anomalous behavior of spectra near phase singularities of focused waves," *Phys. Rev. Lett.* 88, 013901 (2001).

[Pop02] G. Popescu and A. Dogariu, "Spectral anomalies at wave-front dislocations," *Phys. Rev. Lett.* 88, 183902 (2002).

[Gbur02] G. Gbur, T.D. Visser and E. Wolf, "Singular behavior of the spectrum in the neighborhood of focus," *J. Opt. Soc. Am. A* 19, 1694–1700 (2002).

[Foley02] J.T. Foley and E. Wolf, "Phenomenon of spectral switches as a new effect in singular optics with polychromatic light," *J. Opt. Soc. Am. A* 19, 2510–2516 (2002).

[Kiess96] T.E. Kiess and R.E. Berg, "Dominant color reversals and chromaticity cusps in interferometric color mixing," *Am. J. Phys.* 64, 928–934 (1996).

[Hel06] L.E. Helseth, "Spectral density of polychromatic electromagnetic waves," *Phys. Rev. E* 73, 026602 (2006).

[Hlu97] P. Hlubina, "White-light spectral interferometry to measure the effective thickness and the cutting angle of an optical wedge," *Opt. Commun.* 143, 199–203 (1997).

References II

[Kov99] F. Kovacs and A. Csakany, "Spectral interference based accurate measurement of optical thickness," *Opt. Commun.* 165, 143–149 (1999).

[Hlu99] P. Hlubina, "Spatial and temporal coherence of the spectral components of a white-light source in two-beam interference," *J. Mod. Opt.* 46, 1401–1412 (1999).

[Hlu00a] P. Hlubina, "Dispersive spectral-domain two-beam interference analysed by a fibre-optic spectrometer," *J. Mod. Opt.* 47, 1093–1100 (2000).

[Hlu00b] P. Hlubina, "White-light spectral interferometry with the uncompensated Michelson interferometer and the group refractive index dispersion in the interferometer beam splitter," *Opt. Commun.* 175, 293–299 (2000).

[Hlu01a] P. Hlubina, "Spectral-domain intermodal group delay measurement by white-light spectral interferometry," *Meas. Sci. Technol.* 12, 1060–1069 (2001).

[Kov00] F. Kovacs, "Investigation of measurement precision in spectral interference based optical thickness measurement," *Opt. Commun.* 180, 61–68 (2000).

[Farr92] K.B. Farr and N. George, "Beamsplitter cube for white light interferometry," *Opt. Eng.* 31, 2191–2196 (1992).

[Deb06] S.K. Debnath, N.K. Viswanathan and M.P. Kothiyal, "Spectrally resolved phase shifting interferometry for accurate group velocity dispersion measurements," *Opt. Lett.* 31, 3098–3100 (2006).

[Tat81] M. Tateda, N. Shibata and S. Seikai, "Interferometric method for chromatic dispersion measurement in a single-mode optical fiber," *IEEE J. Quantum Electron.* 17, 404–407 (1981).

[Did96] S. Diddams and J.C. Diels, "Dispersion measurements with white-light interferometry," *J. Opt. Soc. Am. B* 13, 1120–1129 (1996).

[HL00] P. Hlubina and J. Luzák, "Differential group refractive index dispersion in optical fibre measured by white-light spectral interferometry," *Opt. Commun.* 180, 329–333 (2000).

[HLU01] P. Hlubina, J. Luzák and W. Urbanczyk, "Spectral-domain intermodal dispersion measurement in a highly birefringent fibre using a Michelson interferometer," *Opt. Commun.* 191, 333–340 (2001).

[Lee06] J.Y. Lee and D.Y. Kim, "Versatile chromatic dispersion measurement of a single mode fiber using spectral white light interferometry," *Opt. Express* 14, 11608–11615 (2006).

References III

[Qi17] W. Qi, X. Huang, D. Ho, S. Yoo, K.T. Yong and F. Luan, "Dispersion measurement of optical fibers by phase retrieval from spectral interferometry," *J. Opt.* 19, 055611 (2017).

[Tap01] J. Tapia-Mercado and A.V. Khomenko, "Precision and sensitivity optimization for white-light interferometric fiber-optic sensors," *J. Lightwave Technol.* 19, 70–74 (2001).

[Khi18] P.P. Khial, A.D. White and A. Hajimiri, "Nanophotonic optical gyroscope with reciprocal sensitivity enhancement," *Nature Photon.* 12, 671–675 (2018).

[Lef22] H.C. Lefevre, *The Fiber-Optic Gyroscope*, Artech House (2022).

[Dor00] C. Dorrer, N. Belabas, J.P. Likforman and M. Joffre, "Spectral resolution and sampling issues in Fourier-transform spectral interferometry," *J. Opt. Soc. Am. B* 17, 1795–1802 (2000).

[Reo06] D. Reolon, M. Jacquot, I. Verrier, G. Brun and C. Veillas, "High resolution group refractive index measurement by broadband supercontinuum interferometry and wavelet-transform analysis," *Opt. Express* 14, 12744–12750 (2006).

[Deng09] Y. Deng, W. Yang, C. Zhou, X. Wang, J. Tao, W. Kong and Z. Zhang, "Wavelet-transform analysis for group delay extraction of white light spectral interferograms," *Opt. Express* 17, 6038–6043 (2009).

[Hlu01FS] P. Hlubina, "White-light spectral interferometry with the uncompensated Michelson interferometer and the group refractive index dispersion in fused silica," *Opt. Commun.* 193, 1–7 (2001).

[Hlu04] P. Hlubina, "Dispersive spectral-domain two-beam interference analysed by a fibre-optic spectrometer," *J. Mod. Opt.* 51, 537–547 (2004).

[Hlu07] P. Hlubina, D. Ciprian, R. Clebus, J. Luňáček and M. Lešňák, "White light spectral interferometric technique used to measure thickness of thin films," *Proc. SPIE* 6616, 661605 (2007).

[Press07] W.H. Press *et al.*, *Numerical Recipes*, Cambridge University Press (2007).

[Palik95] E.D. Palik, *Handbook of Optical Constants of Solids*, Academic Press, Orlando (1995).